Laser Propulsion for Ground to Orbit Launch

Resendes, David; Mota, Sérgio; Mendonça, José; Sanders, Berry; De Teixeira Da Encarnação, J.; Gonzalez del Amo, Jose

Publication date
2005

Document Version
Final published version

Published in
29th International Electric Propulsion Conference

Citation (APA)
Resendes, D., Mota, S., Mendonça, J., Sanders, B., De Teixeira Da Encarnação, J., & Gonzalez del Amo, J. (2005). Laser Propulsion for Ground to Orbit Launch. In *29th International Electric Propulsion Conference* [IEPC-2005-310]

Laser Propulsion for Ground to Orbit Launch

IEPC-2005-310

Presented at the 29th International Electric Propulsion Conference, Princeton University, October 31 – November 4, 2005

David P. Resendes*, Sérgio Mota† and José T. Mendonça‡
Instituto Superior Técnico, Lisboa, Portugal

Berry Sanders§
TNO Prins Maurits Laboratory, Rijswijk, The Netherlands

João Encarnação**
T. U. Delft, Delft, The Netherlands

and

Jose Gonzalez del Amo††
European Space Agency - ESTEC

Ground to orbit launch using laser propulsion requires a thermal system. Physically allowed thermal concepts are discussed and compared. It is argued that the laser supported detonation (LSD) mechanism presents a number of advantages over the alternatives. Numerical simulations of ascent trajectories for a system based on the LSD mechanism were performed to gain insight into the mechanics of laser propulsion and the influence of the most relevant mission parameters. Comparison with the Lightcraft flight data was made and it is shown that the 70 meter height limit is due to excessive laser diffraction. A hypothetical 10 km Lightcraft simulation employing existing technology is presented.

Nomenclature

r	=	radius
Φ	=	latitude
Λ	=	longitude
m	=	mass, mass flow rate
F	=	force resultant
Ω_e	=	earth rotational velocity
I_{sp}	=	specific impulse
η	=	efficiency
θ	=	semi-vertex angle
P	=	power
g_0	=	surface gravitational constant

* Prof., Physics, resendes@ist.utl.pt, AIAA Associate Fellow
† Ph.D. Student, Physics, smota@ist.utl.pt
‡ Full Prof., Physics, titomend@ist.utl.pt
§ Manager, Rocket Technology Group, sanders@pml.tno.nl
** Ph.D. Student, Aerospace, joao.encarnacao@mail.telepac.pt
†† Head, Electric Propulsion Section, jose.gonzalez.del.amo@esa.int

ΔR_{slant} = slant range
C_a, C_n = drag coefficients
T = thrust
λ = wavelength
r_{lsr} = laser main deflector radius
$r_{hot\text{-}spot}$ = vehicle hot spot radius
α_{abs} = atmospheric absorption coefficient
h_{lsr} = laser site altitude
h_{ref} = atmospheric scale height

I. Introduction

While the implementation of a laser thruster may assume different forms, thermal laser propulsive concepts are based on absorption in a *Laser Supported Combustion* (LSC) wave or in a *Laser Supported Detonation* (LSD) wave. These waves are sustained by *Inverse Bremsstrahlung* (IB) absorption after initial ignition. In this process, the laser energy is converted directly to gas translational energy during the (high temperature) spectrally continuous absorption. The resulting hot gases pose two related problems: 1) the gas must be confined without damaging the walls by the heat load; and 2) the heat losses must be minimized. Thermodynamics dictates that only the subsonic LSC wave could be used efficiently in a converging diverging nozzle and the supersonic LSD wave can only be efficiently implemented in a diverging nozzle.

Numerical simulations of laser propulsion were performed to gain insight into the mechanics of laser propulsion ascent trajectories and how these are influenced by the most relevant mission parameters. The simulations were performed using COLVET, a Windows™ application coded in Fortran 95. The vehicle is approximated by a point-mass. There are no moments and the only forces acting on the vehicle are gravity, aerodynamic drag and propulsive thrust. A simple steering program made of steps and slopes performs close to that of optimized pitch programs. This allows for a small number of parameters to completely define a steering program, greatly decreasing the complexity of analyzing laser propulsion.

In section II, the physical mechanisms involved are briefly reviewed. Section III presents the results of flight simulations including comparison with Lightcraft measurements. The final section presents our conclusions.

II. Overview of Thermal Thruster Physics

In a laser thruster, the absorption of laser radiation is coupled to the propellant flow. As in the case of one-dimensional combustion of a premixed fuel/oxidizer combination, the problem of heat addition by absorption of radiation can have two solutions: a subsonic solution (deflagration or combustion branch); and a supersonic solution (detonation branch)[1]. While the implementation of the thruster configuration may assume different forms, thermal laser propulsive concepts with high specific impulse are based on one of these solutions. Steady subsonic flow in an adiabatic variable area channel is possible in a converging nozzle or a diverging diffuser, whereas steady supersonic flow is possible in a diverging nozzle or a converging diffuser. Based on thermodynamic constraints, only the subsonic LSC wave could be used efficiently in a converging diverging nozzle. The supersonic LSD wave can only be efficiently implemented in a diverging nozzle configuration. The geometry of the thruster itself cannot be determined based on thermodynamics alone; fluid mechanics is required.

Thermodynamic constraints limit the LSC wave mechanism to the converging diverging nozzle configuration with laser absorption in the converging part. This requires careful focusing through a throat in the single port configuration (absorption and exhaust channel are the same) or the use of two ports, one for admission of the laser in the converging portion by means of some focusing mirror, and a separate exhaust in the diverging portion. In addition, for constant thrust a *continuous wave* (CW) laser should be used[2,3]. CW LSC (as well as CW LSD) absorption is, however, unstable for the greater part of parameters of interest and is therefore not robust[4]. A pulsed laser is to be preferred. Using a pulsed laser, propulsion based on the LSC mechanism is highly complicated as well as less efficient than the use of the pulsed LSD mechanism, as will be argued below. The pulsed LSD wave mechanism, which can be implemented in the diverging nozzle configuration, is far simpler from a hardware point of view.

Laser supported detonations may be initiated either by direct or by indirect means. In direct initiation, a sufficient amount of energy is deposited rapidly in the mixture resulting in the emergence of a detonation after an initial adjustment period. A simple criterion for direct initiation is that the energy deposited be sufficient to maintain a shock at least as strong as the leading shock of a Chapman-Jouguet wave for a time period at least as long as the

energy deposition time. In indirect initiation, the ignition source is weaker and produces a deflagration, which subsequently undergoes a transition to a detonation. The buildup of pressure waves assumes an important role in promoting this transition which is facilitated by confining the mixture. Pirri studied the LSC to LSD wave transition above metal surfaces[5]. At intensities slightly higher than plasma threshold, a laser supported combustion wave is usually ignited. LSC waves are often seen at intensities from ($2\times10^4 - 10^6$) W/cm^2 for 10.6 μm radiation with both CW and pulsed laser beams. The ignition of a LSC wave initially takes place in the vapour[6,7]. The heated target vapour subsequently transfers its energy to the surrounding air. Once the air begins to absorb a significant fraction of the laser energy, the LSC wave propagates into the air along the beam path. As a consequence of the ignition process and the presence of the target surface, a precursor shock precedes the LSC wave, except at the lowest intensities. A LSC wave propagates into shocked air at very low velocity and thus the absolute wave velocity approximately equals the particle velocity behind the shock. The pressure throughout the region between the wall and the precursor shock remains approximately constant. Since the mass flow through the LSC wave is very low, the plasma temperature is high, leading to strong radiation loss from the plasma.

When the laser intensity is increased, the wave velocity becomes greater than the particle velocity behind the shock since the radiative transfer and the higher temperatures behind a stronger shock result in higher LSC wave speeds. This may be called the weak LSD wave regime where the pressure decreases across the LSC wave. The wave speed relative to the particle speed continues to increase as the laser intensity is increased until the relative particle velocity behind the LSC wave becomes sonic (the Chapman-Jouguet point). The absorption zone now has a velocity equal to the shock velocity and the conditions behind the narrow absorption zone are given by classical LSD wave theory. The laser beam absorption occurs in a thin zone of hot high pressure gas behind the shock wave.

It is found that the maximum energy transfer per unit area transmitted to a surface behind the vapour is obtained when a slowly propagating LSC wave plasma is ignited behind a strong precursor shock in one-dimensional geometry. The pressure is high and so is the temperature because the absolute wave velocity approximately equals the particle velocity, so the mass flow through the LSC is small. The radiation from the plasma is maximized under these conditions. These conditions all favour low propulsion efficiency. When the transition to the LSD wave begins, the mass flow through the absorption zone increases; and increasing the laser intensity further simply partitions more energy into a higher mass flow. The wave propagates faster, but the energy transfer to the surface does not increase. When an LSD wave configuration is ignited, the temperature may actually be lower than for the LSC wave case since the wave is propagating at a higher velocity. Thus in presence of a surface, the LSD mechanism is superior to the LSC mechanism for a propulsion application.

In the pulsed laser propulsion thrusting concept[8], the absorption of laser radiation is typically initiated by focusing the incoming laser beam to produce a laser-induced breakdown of the working fluid just downstream of a nozzle throat, or at the focus of a diverging nozzle. The resulting high pressure plasma continues to absorb laser energy, generating a moving LSD wave. The LSD wave propagates along the beam path and expands down the nozzle. With a short laser pulse, the LSD wave quickly becomes a blast wave which propagates to the nozzle exit plane, converting the high pressure of the propellant gas behind it into a force on the nozzle walls to create thrust. To absorb the laser energy efficiently, the induction time to achieve breakdown should be short compared to the laser pulse duration, and the resulting plasma should be opaque to the laser energy.

LSC and LSD absorption is maintained by Inverse Bremsstrahlung[9]. This is a broadband mechanism in which electrons interact with ions or atoms to absorb laser energy at any wavelength, but with a wavelength dependence which makes absorption at longer wavelengths more favorable. Once the initial electron production is achieved, the LSC or the LSD absorption mechanisms maintain the working fluid at ionization temperatures. The flow rate and size of the wave dictate the amount of gas processed (i.e. thrust) and the efficiency of the processing and expansion through the nozzle dictate the engine performance (i.e. I_{sp}). The initial electron population itself may grow continuously (*continuous absorption*) or abruptly as a sudden flash (*laser induced breakdown*).

We conclude this brief overview, by addressing the issue of ignition of LSC and LSD waves. There are two principal mechanisms for the initial electron generation and growth: *cascade ionization* and *multiphoton ionization* (MPI). The first involves the absorption of laser radiation by electrons when they collide with neutrals (neutral IB). If the few initial electrons gain sufficient energy, they can impact-ionize the gas or solid thereby leading to cascade breakdown in which the electron concentration will increase exponentially in time. For this process to occur there must be an initial electron in the focal volume and then the electrons must acquire an energy greater than the ionization energy of the gas. The second mechanism (MPI) involves the simultaneous absorption by an atom or molecule of a sufficient number of photons to cause its ionization. This mechanism is more effective at shorter laser wavelengths, where the photons are more energetic. Both cascade and multiphoton ionization require high laser intensities, usually in excess of 10^8 W/cm^2. In solids, or in presence of a solid surface, breakdown intensities as low as 10^6 W/cm^2 have been observed. In transparent solids, this has been attributed to nonlinear self-focusing. More

frequently it can be related to microscopic absorption sites (typically impurities), a process which is termed *thermal runaway*.

III. Flight Modeling of Laser Propulsion

Numerical simulations were performed to gain insight into the mechanics of laser propulsion ascent trajectories and how these are influenced by the most relevant mission parameters. The simulations were performed using COLVET[10], a Windows™ application coded in Fortran 95. The following equations of motion are integrated using a Runge-Kutta algorithm:

$$\begin{aligned}
\ddot{r} &= \tfrac{F_r}{m} - r\dot{\Phi}^2 - r\left(\dot{\Lambda}+\Omega_e\right)^2\cos^2\Phi \\
\ddot{\Lambda} &= \tfrac{1}{r\cos\Phi}\left[\tfrac{F_\Lambda}{m} + 2\dot{r}\left(\dot{\Lambda}+\Omega_e\right)\cos\Phi + 2r\dot{\Phi}\left(\dot{\Lambda}+\Omega_e\right)\sin\Phi\right] \\
\ddot{\Phi} &= \tfrac{1}{r}\left[\tfrac{F_\Phi}{m} - r\left(\dot{\Lambda}+\Omega_e\right)^2\sin\Phi\cos\Phi - 2\dot{r}\dot{\Phi}\right]
\end{aligned} \tag{9}$$

The vehicle is approximated by a point-mass. There are no moments and the only forces acting on the vehicle are gravity, aerodynamic drag and propulsive thrust, which are added to produce the force components F_r, F_Λ and F_Φ. Thrust attitude is set with the steering angles. The simulations take place over a spherical, non-rotating Earth, using the standard atmospheric model. The drag model is the same as in Ref. 11, with α the angle between the velocity vector and the thrust vector:

$$\begin{aligned}
C_{axial} &= 2\sin^2\theta_s + \sin^2\alpha(1-3\sin^2\theta_s) \\
C_{norm} &= \sin 2\alpha\cos^2\theta_s
\end{aligned} \tag{10}$$

The semi-vertex angle, θ_s, is taken to be 55 degrees. Thrust is generated from a laser beam hitting the vehicle's hot-spot following the law:

$$T = \frac{2\eta_{thr}P_{thr}}{I_{sp}g_0} \tag{11}$$

The thrust efficiency, η_{thr}, models the losses during the conversion of the energy conveyed by the laser photons to propulsive power. The propulsive power, P_{thr}, is the fraction of the initial laser power that reaches the vehicle:

$$P_{thr} = \eta_{atm}\eta_{diff}P_{lsr} \tag{12}$$

The losses are mainly due to two factors: diffraction and atmospheric absorption.

$$\eta_{diff} = 1 - 4\left(\Delta R_{slant}\frac{\lambda_{lsr}}{2\pi r_{lsr}r_{hot-spot}}\right) \tag{13}$$

$$\eta_{atm} = \exp\left(-\alpha_{abs}\left(e^{-h_{lsr}/h_{ref}} - e^{-h/h_{ref}}\right)\frac{h_{ref}}{\cos\theta_{lsr}}\right) \tag{14}$$

with h_{ref} = 8000m. An important parameter in laser propulsion is the laser intensity on the vehicle:

$$I_{lsr} = \frac{P_{thr}}{\pi r_{hot-spot}^2} \tag{15}$$

Benchmarking was performed with the validations aiming at reproducing the same trajectories as close as possible. It is never possible to duplicate every single calculation, since different computer programs work

differently as well as the fact that laser-propelled launches depend heavily on the position of the vehicle, which naturally leads to using different control variables than used in traditional chemical rockets. A good example of this is the steering program, which in laser propulsion uses mostly the incidence angle (angle between the transmitted laser beam and the base of the vehicle) as opposed to the pitch angle (angle between the thrust vector and the local horizontal plane). Instead of implementing a dedicated steering program, the trajectories were reproduced using a *targeting* or *fitting* strategy. This basically involves using the conventional pitch angle in simple evolutions (steps and slopes) to fit the resulting trajectory to that of the validating simulation. The criterion for a successful validation then becomes the evolution of the state variables - position, velocity, acceleration, time and mass. Validation against Humble and Pierson[11] was quite satisfactory.

Simulations on experimentally available data are treated next. Ground-breaking flight work on Laser Propulsion has been carried out by Leik Myrabo [12]. The mission details appear in Table 1.

Launch mass	50.62	g	
Diameter	12.2	cm	
Laser power	10	kW	
Laser wavelength	10.6	nm	
Flight time	12.7	s	
Drag coefficient	0.7		estimated
Specific impulse	850	s	estimated
Thrust efficiency	40%		estimated
Main reflector diameter	1.0	cm	estimated

Table 1. Myrabo-like laser propulsion vehicle and laser

Some parameters were guessed which allowed for some fitting of the experimental data to the simulations thus confirming the guesses. Figure 1 compares altitude and velocity with the data available in [12], which is only valid for the first six seconds of the flight. The simulation is remarkably close to experimental results. The vehicle reaches zero vertical velocity, exactly 12.7 s after launch at the hovering altitude of 71.3 m as reported in [12]. The initial acceleration phase, up to 2 seconds into the flight, is reproduced in the velocity profile. The altitude seems to be shifted vertically by a few meters but the linear evolution is mirrored. It is also possible that the experimental altitude measurements did not have the ground as reference. The vehicle stops climbing although the laser continues to operate because of low diffraction efficiency which drops off to about 40% at the end of the flight. The distance at which the laser power on the vehicle drops to zero due to diffraction is just about 90 m and hence there is no thrust above this altitude. This may account for the lack of success that Myrabo has encountered in taking his vehicles higher than 70 m. Drag is also of paramount importance. The peak drag, occurring roughly 3 seconds into the flight, amounts to about half of available thrust. Had this vehicle been meant for higher velocities, it would need a very efficient aerodynamic shape. Thrust decreased monotonically from 1 to 0.4 N. Mass remained essentially constant during the flight as did the pitch angle and atmospheric absorption.

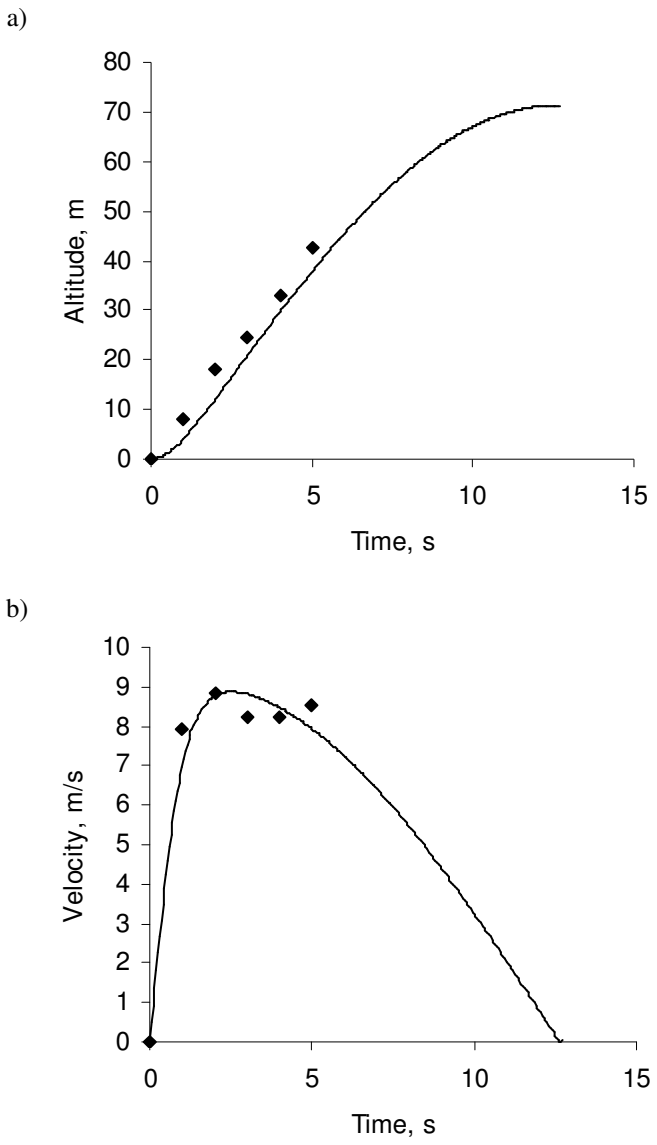

Figure 1. Profile comparison with Myrabo flight results: a) altitude and b) velocity

Additional simulation under the conditions of this calculation, but without diffraction, show that indeed laser diffraction is height limiting. Upon its elimination the vehicle will reach nearly 115 m in height, at which point thrust equals drag. Further height performance can still be achieved by optimizing vehicle drag.

Future experimental work should aim at taking a small vehicle, such as the one used by Myrabo, to several kilometers in altitude. Since that altitude will be most likely reached in a vertical ascent, the present analysis can be applied to this case. For the sake of clarity, this hypothetical flight will be called second generation laser propulsion.

The assumptions for this hypothetical case are indicated in Table 2.

Launch mass	500	g
Target altitude	8	km
Laser power	100	kW
Main reflector diameter	100	cm

Table 2. Second generation of Myrabo-like laser propulsion

The vehicle is essentially identical as before. The important difference is that the scale of the ascent is larger, at the expense of a tenfold increase in laser power and vehicle launch mass and widening the beam width a hundred-fold to a meter. It is expected that even further increase in performance is attainable if the proper vehicle design is undertaken. One hundred kilowatt average power is currently state-of-the-art using CO_2 gas laser technology[13]. The simulation results are summarized in the following plots.

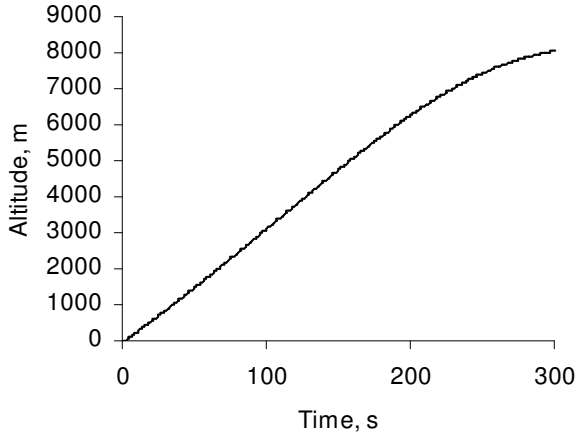

Figure 2a. Second generation Myrabo-like laser propulsion: Altitude

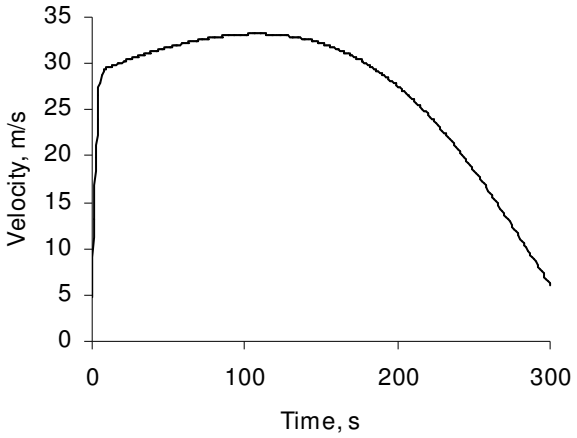

Figure 2b. Second generation Myrabo-like laser propulsion: Velocity

The mass consumption in the experimental flight was calculated at about 100 g; while for the second generation it amounts to about 2.36 kg. This mass is ablated material from the vehicle. An altitude of 8.04 km is reached in approximately 300 seconds. The velocity increase is sharp at the beginning of the flight, saturates and decreases subsequently. Atmospheric transmission efficiency remains above 90%. However, the diffraction efficiency at maximum height is but one third of its value at ground level. Thrust decreases monotonically from 9.6 N to about 2.6 N. At maximum velocity, thrust equals drag plus vehicle weight. The simulation indicates that laser flights to a few kilometers are possible with existing technology.

IV. Conclusions

For a ground to orbit launch, only a thermal thruster concept is viable. Non-equilibrium concepts involving very short laser pulses, up to 10^{-12} s, while very attractive from a specific impulse perspective, have thrust levels many orders of magnitude below the requirements for ground to orbit launch and are incompatible with hydrodynamic time scales. Of the thermal concepts/technologies studied, the most promising is the LSD (Laser Supported Detonation) wave mechanism, either the air breathing or rocket mode. The LSD generates higher I_{sp} and higher thrust. Full advantage of laser propulsion requires that higher specific energies be deposited in the propellant.

The LSD mechanism, and quite generally other plasma absorption mechanisms, require prompt uniform ignition. This can be achieved either by laser focusing or by using a low temperature ionization mechanism. To protect walls from the high temperatures reached, in the (10 000–20 000) K range, it is important to use ablative material on sensitive surfaces. Laser beam steering for laser propulsion can be successfully implemented by passive stabilization in which the launch vehicle "searches" for the laser beam, so called "beam riding". The thruster should be designed so that axial deviations are stabilized by the propellant flow configuration. Transverse stabilization can be achieved by requiring that the center of thrust be ahead of the center of drag.

From ballistics considerations alone, there is a minimal laser power that will launch a given mass. Small vehicles have limited launch ranges due to drag effects. Aerodynamic design should be a major design driver. Current available state-of-the-art laser power levels, of the order of 100 kW in CW mode for CO_2 lasers, will allow launching of 200 g in mass to above 10 km in height. The concurrent optics are available. There is a threshold mass and size to get to orbit. For LEO, simulations indicate that the minimal size is 3 kg using a 3 MW laser.

Acknowledgments

The authors acknowledge the financial support of the European Space Agency (ESA) through contract 17048/03/NL/PA "Laser Propulsion for ESA Missions: Ground to Orbit Launch".

References

[1]Forman Williams, Combustion Theory 2nd Ed., Benjamin Pub. Co., 1985

[2]Kemp, N. H. and Krech, R. H.. "Laser-Heated Thruster Final Report," NASA CR-161665 (PSI TR-2220), Physical Sciences Inc., Andover, Mass., September 1980. See also: AIAA Paper No. 811249.

[3]Legner, H.H. and Douglas-Hamilton, D. H., "CW Laser Propulsion", Journal of Energy, Vol. 2, March-April 1978, pp.85-94.

[4]Wu, P.K.S. and Pirri, A.N., "Stability of Laser-Heated Flows," AIAA Journal, vol. 14, March 1976, pp. 390-392.

[5]A.N. Pirri, R.G. Root, and P.K.S. Wu, "Plasma Energy Transfer to Metal Surfaces Irradiated by Pulsed Lasers", AIAA J. vol. 16, pp. 1296 (1978).

[6]Boni, A. A., Su, F. Y., Thomas, P.D., and Tdusal, H. M., "Theoretical Study of Laser-Target Interactions," Mid-Term Tech. Rept. SAI 76-722-LJ, Science Applications Inc., La Jolla, Cà1if., Aug.1976.

[7]Pirri, A. N., "Analytic Solutions for Laser-Supported Combustion Wave Ignition Above Surfaces," AIAA Paper 76-23, Washington, D.C., Jan. 1976.

[8]Rosen, D. L, Kemp, N. H., Weyl, G., Nebolsine, P. E., and Kothandaraman, R., "Pulsed Laser Propulsion Studies Vol I, Thruster Physics and Performance," PSI TR-184, Physical Sciences Inc., Andover, Mass., 1982.

[9]Caledonia, G. E., Wu, P. K. S., and Pirri, A. N" "Radiant Energy Absorption Studies for Laser Propulsion," NASA CR-134809 (PSI TR-20), Physical Sciences Inc., Andover, Mass" March 1975, see also Journal of Energy, Vol. I, March-April 1977, pp. 121-124.

[10]João Encarnação, Numerical Simulations of Ascent Trajectories", Thesis, Delft Aerospace, U. Delft, 2005.

[11]W. Edward Humble; Bion L. Pierson. Maximum-paylod trajectories for a laser-propelled vehicle. Vol. 18, no. 6, Journal of Guidance, Control and Dynamics, 1995.

[12]Leik N. Myrabo. Brief history of the ligthcraft technology demonstrator (ltd) project. Technical report, Rensselaer Polytechnic Institude, 2001.

[13]Rodin, A.V., Naumov, V.G., Nastoyashchii, A.F., and Shashkov, V.M., "High Energy Pulse-Repetitive CO2 Laser for Lightcraft Experiments," 1st Int. Symp. on Beamed Energy Propulsion, Huntsville, Al., 2002, ed. A. Pakhomov, AIP Conf. Proc. 664, pp. 612.